

Theoretical and experimental aspects of chaos control by time–delayed feedback

Wolfram Just^{1)*†}, Hartmut Benner²⁾, and Ekkehard Reibold²⁾

¹⁾Institut für Physik, TU Chemnitz, D-09107 Chemnitz, Germany

²⁾Institut für Festkörperphysik, TU Darmstadt,
Hochschulstr. 6, D-64289 Darmstadt, Germany

May 14, 2002

Abstract

We review recent developments for the control of chaos by time–delayed feedback methods. While such methods are easily applied even in quite complex experimental context the theoretical analysis yields infinite–dimensional differential–difference systems which are hard to tackle. The essential ideas for a general theoretical approach are sketched and the results are compared to electronic circuits and to high power ferromagnetic resonance experiments. Our results show that the control performance can be understood on the basis of experimentally accessible quantities without resort to any model for the internal dynamics.

Control of chaos, i.e. the stabilisation of unstable states by non-invasive methods, has become one of the most rapidly developing branches in applied nonlinear science. From the point of view of applications time–delayed feedback methods are very popular control schemes, since they can be used in quite different experimental contexts. We review recent analytical results concerning the universal properties of time–delayed feedback control. The theoretical predictions concerning e.g. the control thresholds are confirmed by electronic circuit experiments and explain the control behaviour in high–power ferromagnetic resonance experiments. Some implications for control of spatio–temporal chaos are described, in particular the role of spatio–temporal filters for the improvement of the control performance.

*e-mail: wolfram.just@physik.tu-chemnitz.de

†permanent address: School of Mathematical Sciences, Queen Mary / Univ. of London, Mile End Road, London E14NS, UK

1 Introduction

The influence of time dependent perturbations on the dynamical behaviour is still one of the most fascinating problems in natural sciences and engineering. Although the importance and relevance of resonance phenomena are known for centuries, the development of Nonlinear Dynamics has led to new aspects during the last decade. Particular milestones are the problem of synchronisation in dynamical systems [1] and the selection and stabilisation of unstable states by tiny driving fields [2]. While the first concept has meanwhile led to new notions of synchronised motion and plays a role e.g. in branches like coding theory, the second concept, usually called chaos control, has proven to be fruitful in quite different branches of applied sciences [3].

Problems of control are of course a classical discipline in engineering science and applied mathematics and have been investigated for at least half a century (cf. e.g. [4]). The new aspect introduced recently was the emphasis of non-invasive control, i.e. control methods where the control force vanishes asymptotically whenever imperfections like thermal noise can be neglected. Such schemes are relevant if one stabilises proper unstable states of the dynamical system. The solution of a control problem is quite simple, in principle. One just has to turn all the unstable eigenmodes of a state into stable modes. Such a concept is often called pole placement technique. The strategy proposed in [2] was based on geometric considerations valid in the vicinity of the state to be stabilised.

In the wake of the pioneering work [2] a whole industry of chaos control papers developed (cf. e.g. [5]). But the original control method contains a main flaw often relevant in applications. The control scheme requires some information about the internal dynamics either by a mathematical model or some phase space reconstruction technique (e.g. [6]). In fact, under such circumstances traditional control theory is very efficient although the handling of time dependent target states often poses some challenge. The situation becomes much worse if no modeling of the dynamics is possible. Control schemes have been proposed which might cope with situations where no modelling is possible (e.g. [7]). But they are often just slight extensions of classical concepts known by engineers for quite a while. In fact, some of these approaches are invasive methods in contrast to what has been mentioned in the literature [8].

A real new idea for stabilising time periodic states by a non-invasive method was based on the observation that proper control forces can be generated by time-delayed differences of measured signals [9]. Such a method can easily be implemented in quite complex experiments, since the basic idea is simple and does not need any modelling of the internal dynamics. Let us assume we have a dynamical system or an experiment where the vector $\mathbf{x}(t)$ denotes the complete mesoscopic state of the system. Of course we do not know the state explicitly. We are just able to measure a (scalar) signal $s(t) = g[\mathbf{x}(t)]$ which depends on the internal state in some unknown way. Let $\boldsymbol{\xi}(t) = \boldsymbol{\xi}(t + \tau)$ denote the periodic

unstable state which we intend to stabilise. The key idea of time–delayed feedback control consists in imposing a force on the system which is proportional to the time–delayed difference of the measured signal, $\Delta s(t) = s(t) - s(t - \tau)$. Provided that the delay time τ coincides with the period of the orbit the control scheme satisfies at least the constraint that the force vanishes when the target state $\xi(t)$ is reached, i.e. the method yields a non–invasive control scheme. At the moment we assume for simplicity that the period of the orbit is known in advance, so that the delay time can be adjusted properly. The whole control setup is sketched in figure 1.

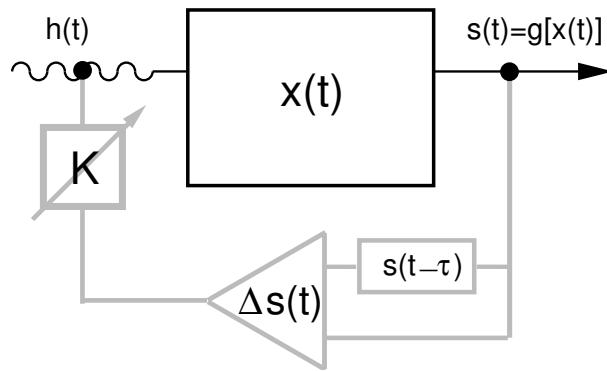


Figure 1: Control scheme for time–delayed feedback control. The control loop is displayed in gray. The control force consists of the control signal $\Delta s(t)$ and the control amplitude K which acts as a linear amplification.

Temporal delays are quite easy to realise in real experiments. One may either use analog delay lines, digital computers, or just the signal travelling times through cables or optical resonators. For a theoretical analysis of the control performance one has to convert the information of the control scheme displayed in figure 1 into an equation of motion without referring to a particular experimental context. Thus we obtain

$$\dot{\mathbf{x}}(t) = f(\mathbf{x}(t), K\Delta s(t)) \quad (1)$$

where the dependence of the right hand side on the internal degrees of freedom and on the control force $F(t) = K\Delta s(t)$ cannot be specified without further knowledge. The time–delayed feedback scheme according to the original idea of Pyragas, however, tells us that the control force reads

$$F(t) = K\Delta s(t) = K(g[\mathbf{x}(t)] - g[\mathbf{x}(t - \tau)]) \quad . \quad (2)$$

From the theoretical point of view eqs.(1) and (2) have to be analysed with respect to stabilising a particular periodic state $\xi(t)$. In that context the control

amplitude K plays the role of the relevant experimental parameter which has to be adjusted properly.

2 Control performance

For the theoretical analysis of eq.(1) we have to assume that the free system, i.e. eq.(1) for $K = 0$, has an unstable time periodic state $\boldsymbol{\xi}(t)$ with period τ . Following the original idea of chaos control such states typically exist in chaotic systems where periodic solutions are embedded in the chaotic attractor, although from the point of view of control such a chaotic environment is not a necessary condition. Thus the free systems has a solution $\boldsymbol{x}(t) = \boldsymbol{\xi}(t) = \boldsymbol{\xi}(t-\tau)$. Employing the stability of the system subjected to control we resort to the usual linear stability analysis by considering a small neighbourhood of our target solution, $\boldsymbol{x}(t) = \boldsymbol{\xi}(t) + \delta\boldsymbol{x}(t)$. For small increments $\delta\boldsymbol{x}(t)$ the full system (1) and (2) results in a linear differential–difference equation

$$\delta\dot{\boldsymbol{x}}(t) = D_1f(\boldsymbol{\xi}(t), 0)\delta\boldsymbol{x}(t) + KM(\boldsymbol{\xi}(t))(\delta\boldsymbol{x}(t) - \delta\boldsymbol{x}(t - \tau)) \quad (3)$$

where D_1f denotes the Jacobian of the free system and the control matrix M is given in terms of derivatives of the dynamics with respect to the control force and of the measured quantity

$$M(\boldsymbol{\xi}) = d_2f(\boldsymbol{\xi}, 0) \otimes dg[\boldsymbol{\xi}] \quad . \quad (4)$$

The linear system (3) can be solved by expansion in terms of eigenmodes

$$\delta\boldsymbol{x}(t) = \exp[(\Lambda + i\Omega)t]\boldsymbol{U}(t) \quad . \quad (5)$$

Via the motion along the periodic state our system is periodically time dependent. Thus the Floquet decomposition applies which tells us that the eigenmodes are periodically time dependent as well, $\boldsymbol{U}(t) = \boldsymbol{U}(t - \tau)$. Stability of the state is governed by the real part of the Floquet exponent $\Lambda + i\Omega$, where indices numbering the different exponents have been suppressed for simplicity. Owing to the periodicity of the eigenmode the delay disappears from the full system (3) when the ansatz (5) is employed. The contribution from the control matrix contains the eigenvalue as a parameter, and one ends up with the usual Floquet eigenvalue problem

$$(\Lambda + i\Omega)\boldsymbol{U}(t) + \dot{\boldsymbol{U}}(t) = [D_1f(\boldsymbol{\xi}(t), 0) + K(1 - \exp[-(\Lambda + i\Omega)\tau])M(\boldsymbol{\xi}(t))]\boldsymbol{U}(t) \quad . \quad (6)$$

Such nonlinear eigenvalue problems usually yield transcendental characteristic equations [10]. For a numerical evaluation one requires of course the explicit form of the free Jacobian D_1f and of the control matrix M . There exist nice approaches based on complex contour integrals where numerical exact statements

about the spectrum and in particular about the stability can be derived [11]. But the emphasis of delayed feedback control is on systems where no model equations are available. Even without knowing the analytical form of the control matrix and of the free Jacobian properties of the eigenvalue problem can be evaluated. For the onset of stability the real part Λ has to change its sign. One can prove that such a case happens only if the imaginary part Ω is nonzero [12]. Furthermore stabilisation is impossible when the orbit $\xi(t)$ of the free system has an even number of real Floquet exponents [13]. Such constraints can be visualised by a geometric argument [14]. One needs torsion in the neighbourhood of the desired orbit in order that time-delayed feedback methods work at all. Such a topological constraint explains why the method may fail in certain dissipative low-dimensional systems.

For a numerical evaluation of the eigenvalue problem (6) one has to resort to approximations. Using a perturbative approach by expanding in terms of the control amplitude the characteristic equation of eq.(6) can be written as [12]

$$\Lambda + i\Omega = \lambda + i\omega + (\chi' + i\chi'')K (1 - \exp[-(\Lambda + i\Omega)\tau]) \quad . \quad (7)$$

Here $\lambda + i\omega$ denotes the Floquet exponent of the free orbit, and the complex valued parameter $\chi' + i\chi''$ takes all the details of the control scheme into account. In practice these numbers may be considered as fit parameters. For a detailed discussion of the approximation leading to eq.(7) we refer to [15]. We just mention that eq.(7) becomes an exact expression for a particular choice of the control matrix, namely diagonal control where each degree of freedom is measured and controlled so that M becomes the identity matrix.

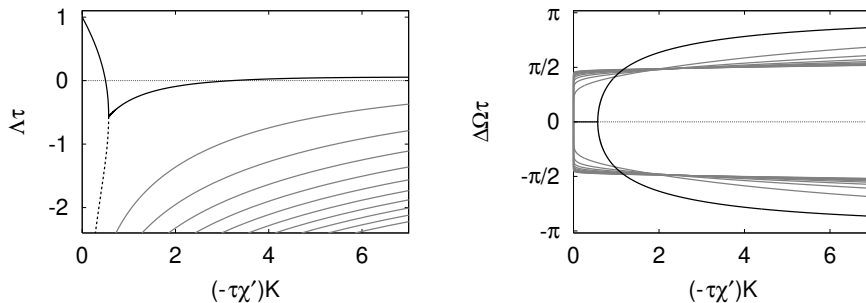


Figure 2: Dependence of the real part Λ of the Floquet exponent and of the frequency deviation $\Delta\Omega = \Omega - \omega$ on the control amplitude for $\lambda\tau = 1$ (theoretical prediction according to eq.(7)). Full line: dominant eigenvalue, gray: non-leading part of the spectrum.

Evaluation of the transcendental equation (7) is now straightforward. We just consider the special case of orbits which flip their neighbourhood during one turn,

i.e. $\omega\tau = \pi^1$. Figure 2 contains the dependence of real and imaginary part on the control amplitude. One obtains a characteristic butterfly shaped curve for the real part which results in a finite control interval where $\Lambda < 0$. That behaviour is accompanied by a frequency splitting phenomenon for the imaginary part, caused by a collision of two distinct Floquet exponents. The whole spectrum consists of an infinite number of eigenvalues, reflecting the infinite-dimensional nature of the differential-difference equation (3). However, all these nonleading eigenvalues have negative real parts and do not contribute to the control performance.

Such a theoretical prediction can be compared with experiments where the stability exponents are accessible. Typically such a situation occurs in simple demonstration experiments like electronic circuits. A simple non-autonomous example is the nonlinear diode resonator illustrated in figure 3. Here the periods of the unstable orbits are known a priori, since they are given by integer multiples of the period of the driving voltage. Without control the system undergoes a period doubling cascade to chaos on variation of the driving amplitude U_A . This guarantees a nonzero torsion ($\omega = \pi/\tau$) of the unstable periodic orbits.

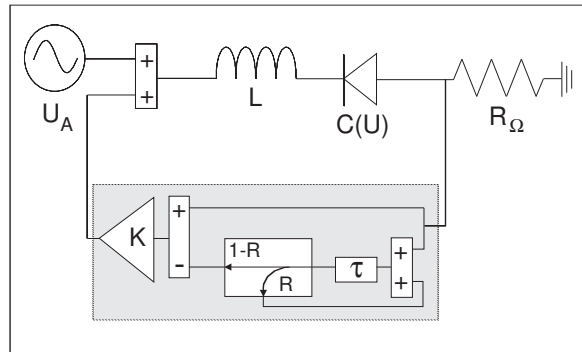


Figure 3: Experimental setup of the nonlinear diode resonator with extended time delay feedback device.

The Floquet exponents can be measured e.g. by employing linear response methods. Here one superimposes a small harmonic additional forcing and detects the control signal. The corresponding Fourier spectrum within the control regime is shown in figure 4. The positions and widths of the lines yields the imaginary and real parts of the corresponding Floquet exponent. The general theory fits well with experimental results (cf. figure 5), even a quantitative coincidence of up to 5% is observed.

¹Such a choice implies $\chi'' = 0$, cf. e.g. [12].

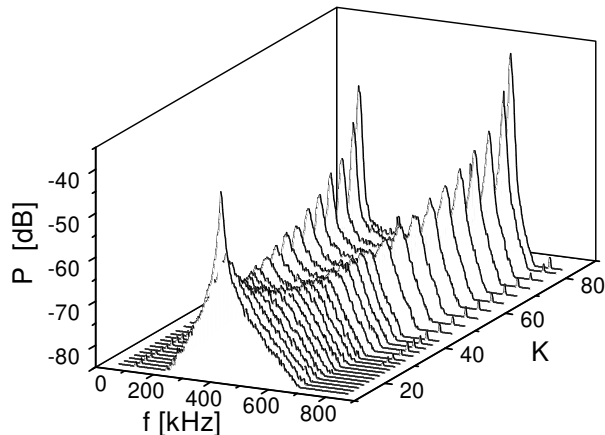


Figure 4: Response spectrum of an electronic circuit subjected to delayed feedback control within the control domain. Peaks are caused by the leading Floquet exponent.

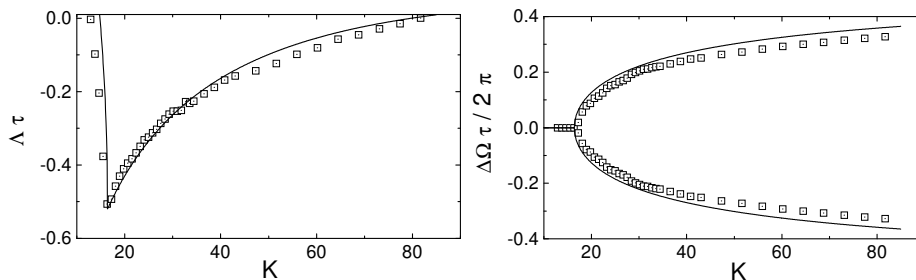


Figure 5: Real and imaginary part of the leading Floquet exponent in dependence on the control amplitude K for an electronic circuit experiment. Symbols: experimental results, line: numerical fit according to eq.(7) with $-\tau\chi' = 0.036$ and $\lambda\tau = 1.07$.

The typical shape of the leading eigenvalue yields a finite control interval with two thresholds, a lower and an upper critical control amplitude. At the lower threshold control sets in via a reversed flip bifurcation. Provided the bifurcation is supercritical one expects that in the Fourier spectrum of the measured signal a peak at half the basic frequency disappears when one enters the control interval by changing K . This prediction is confirmed in experiments (cf. figure 6). At the upper threshold the eigenvalue spectrum has developed a nontrivial imaginary part indicating a Hopf bifurcation. Thus sideband frequencies are observed in the Fourier spectrum of the signal. Both features are typical for time-delayed feedback methods.

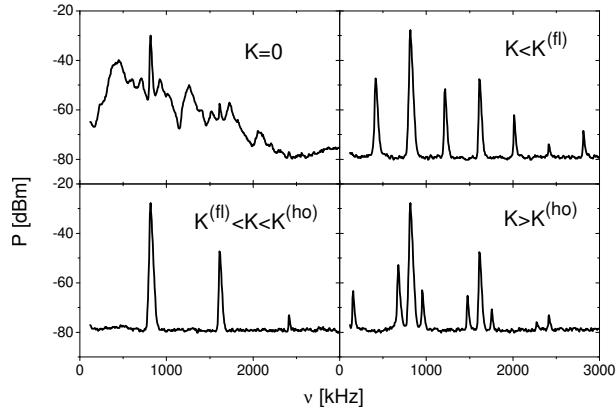


Figure 6: Fourier spectrum of the measured signal, without control ($K = 0$: chaotic), below the lower critical control amplitude ($K < K^{(fl)}$: period two), within the control interval ($K^{(fl)} < K < K^{(ho)}$: periodic), and above the upper control threshold ($K > K^{(ho)}$: quasiperiodic).

The size of the control interval depends on properties of the free orbit, in particular on its Lyapunov exponent λ . On increasing λ the spectrum displayed in figure 2 is essentially shifted upwards. A more thorough analysis shows [16], that the control interval vanishes when $\lambda\tau = 2$. Such a constraint limits the original scheme according to eq.(2) to weakly unstable orbits. Altogether the analytical approach described here allows to detect the strenght and weakness of time-delayed feedback control.

3 Control in strongly driven magnetic systems

High power ferromagnetic resonance experiments were performed on spheres of yttrium iron garnet (YIG), which is well established as a "prototype nonlinear ferromagnet". The parametric excitation of spin waves was observed in *subsidiary absorption* and *parallel pumping* (cf. e.g. [17]). The sample was placed in a microwave cavity and excited by a microwave field of frequency ν , applied perpendicularly or parallel to the static magnetic field (cf. figure 7). The subsidiary absorption manifests as an additional absorption structure at lower field, which is well separated from the FMR main resonance and shows a drastic broadening with increasing microwave power, accompanied by auto-oscillations and sequences of bifurcations. We have systematically analysed [18] the dynamic behaviour of the subsidiary absorption signal at fixed pumping frequency, as presented for instance in figure 8.

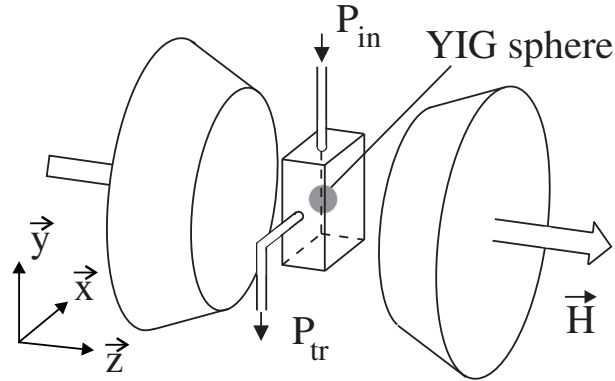


Figure 7: Setup for the ferromagnetic resonance experiment.

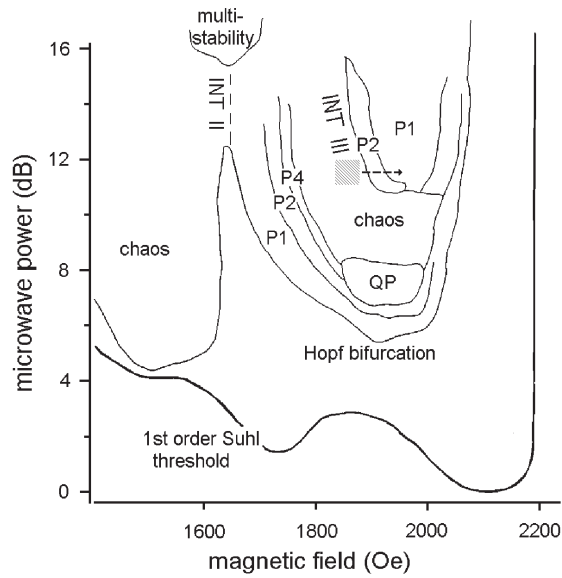


Figure 8: Experimental bifurcation diagram for high-power ferromagnetic resonance on a YIG sphere ($\nu = 9.26\text{GHz}$) with respect to magnetic field H and input microwave power P_{in} . The lowest line indicates the Suhl threshold, the lines above separate regimes of different time behaviour, e.g. period doublings (P2, P4), quasiperiodicity (QP), different types of intermittency (INT II, III) or chaos.

It is a characteristic feature of these strong nonequilibrium ferromagnetic resonance experiments that the absolute values of magnetic fields, i.e. the location

of bifurcation lines in the diagram 8, depend sensitively on the details of the magnetic experiment, in particular on the magnon damping, the surface roughness of the sample, the orientation of the crystal axis, and the electric coupling and the quality factor of the cavity. These properties differ from setup to setup but the topology of the bifurcation diagram does not depend on these features. Thus one has to be careful when comparing directly the absolute values of critical and static fields of different experimental setups. Usually deviations of several 10Oe appear between different types of experiments.

The lower line in figure 8 shows the dependence of the Suhl threshold on H (the so-called *butterfly curve*)². The next line indicates a Hopf bifurcation and corresponds to the onset of auto-oscillations. Further bifurcation lines at higher input power separate regimes of different time behaviour, e.g. period doublings, quasiperiodicity, different types of intermittency or chaos. The auto-oscillation frequencies were in the MHz range and changed dramatically on variation of system parameters, thus making the τ adjustment a challenge. For the given setup (cf. figure 9) an intrinsic control loop latency of about 70ns was observed.

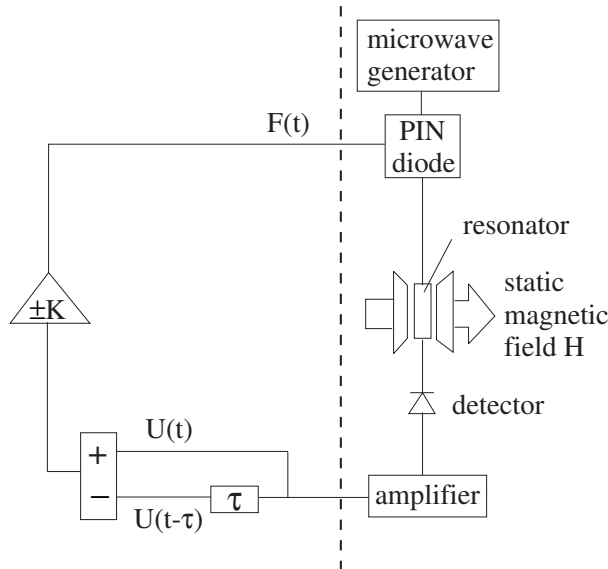


Figure 9: Experimental control of the ferromagnetic resonance experiment by time-delayed feedback.

To illustrate the applicability of the delayed feedback control method to complex spin systems, as a first step we considered a *stable* period-2 orbit (figure 10, $K = 0$), which was generated through a period doubling, leaving an unstable period-1 orbit with flipping neighbourhood ($\omega = \pi/\tau$). This unstable

²Here and in the corresponding figures below P_{in} was normalized to the minimum threshold.

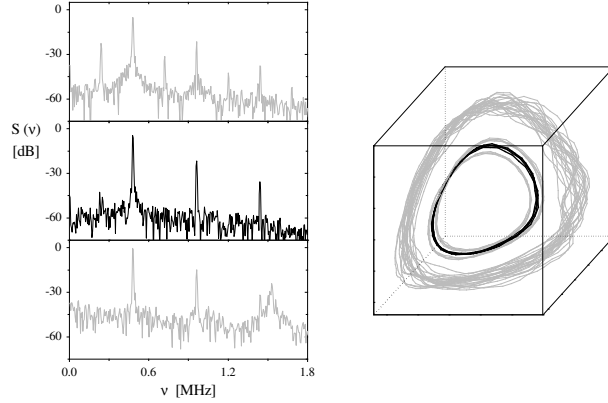


Figure 10: Suppression of a period-2 orbit (parallel pumping, $\nu = 9.39\text{GHz}$, $P_{in} = 13.3\text{dB}$, $H = 1613\text{Oe}$). When comparing the data to the diagram 8 one has to take into account that the pump frequencies differs by 1.4%. L.h.s. top to bottom: stable period-2 orbit ($K = 0$), controlled period-1 orbit ($K = 0.2$), feedback induced torus ($K = 0.5$). R.h.s.: corresponding phase space representations using delay embedding. Note that the stabilised UPO (dark) is located close to the starting period-2 orbit, while for large K an attractor widening occurs.

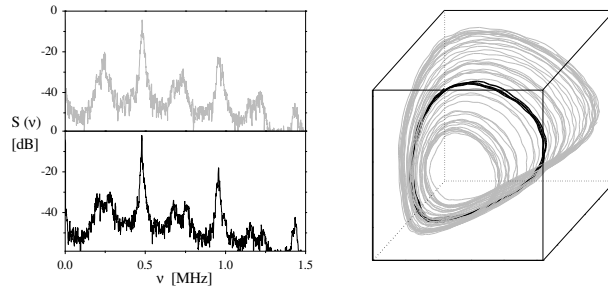


Figure 11: Suppression of chaos (subsidiary absorption, $\nu = 9.39\text{GHz}$, $P_{in} = 8.5\text{dB}$, $H = 1865\text{Oe}$). L.h.s. top to bottom: chaotic attractor ($K = 0$), stabilised period-1 orbit ($K = 0.37$). R.h.s.: corresponding phase space representations. Note that the stabilised periodic orbit (dark) is embedded in the chaotic attractor.

orbit was selected for control. The delay time $\tau = 2.09\mu\text{s}$ was evaluated from the very sharp and dominating peak in the spectrum. Turning on the feedback and increasing the control amplitude K , we observed a changeover to period-1 (figure 10, $K = 0.2$), while the period-2 component was suppressed by more than 20dB. The vanishing control signal (below a noise level of about 1% of the diode signal) indicated successful control. On further increase of K , the orbit was destabilised again. A widening of the attractor occurred, accompanied by a Hopf bifurcation³ which resulted in an additional broad peak at about 1.53MHz (figure 10, $K = 0.5$). According to the theoretical expectations, there is a K -window of successful control which is limited at low K -values by a flip bifurcation and at high K -values by a Hopf bifurcation.

In order to extend these control experiments to the chaotic regime we looked for a parameter range where chaos evolves via a period doubling, leading to a flipping neighbourhood ($\omega = \pi/\tau$). However, this period doubling was followed by two Hopf bifurcations making the the situation more complex. A proper starting value for the cycle time $\tau = 2.08\mu\text{s}$ was obtained from the unperturbed spectrum, (figure 11, $K = 0$). We tried to improve this value by applying the sophisticated iterative procedure described in [19], but the control signal remained nearly unaffected. The unperturbed spectrum again showed a noisy but distinct period-2 component. When applying a moderate feedback amplitude ($K = 0.37$), the irregular behaviour was largely suppressed (figure 11). The period-1 peak became rather narrow, the period-2 fluctuations were decreased by about 15dB, whereas the frequency components resulting from the Hopf bifurcations were less affected.

These experiments show that chaotic spin systems, in spite of their complexity and fast time scale, can be controlled by time-delayed feedback technique. General properties and limitations of this technique, as predicted from a system-independent theory, show up very distinctly in our experimental findings.

4 Spatio-temporal control

The approaches described in section 2 apply to any dynamical system, i.e. to spatially extended systems as well. Experimental aspects have been mentioned in the previous section. However, the plain control method does not take the properties of spatial degrees of freedom explicitly into account. Any modification of the control method should be simple enough that an application in fairly complicated experimental situations is still possible. A method which aims at such a goal is the application of Fourier decomposition in order to achieve stabilisation in extended systems with large aspect ratio [20]. Fourier decomposition can be performed by simple devices in optical experiments. A feedback of certain Fourier

³Additional secondary instabilities [15] appear in the experiment on increasing K , so that the resulting torus does not wrap around the unstable periodic orbit.

modes which represent the desired pattern may lead to non-invasive control of spatially periodic and regular states in certain laser experiments [21]. To some extent such methods use a spatial delay to achieve stabilisation.

To shed more light in a systematic way on such approaches let us dwell on some theoretical background from the point of view of delayed feedback control. Let $\mathbf{x}(t)$ denote the state of the system, where the vector \mathbf{x} may be a high-dimensional object including spatial variables as well. The free motion without control is assumed to obey the set of equations

$$\dot{\mathbf{x}}(t) = f(\mathbf{x}(t)) \quad . \quad (8)$$

Stability of the pattern $\boldsymbol{\xi}(t) = \boldsymbol{\xi}(t + \tau)$ is determined by the linear eigenvalue problem

$$(\lambda + i\omega)\mathbf{u}(t) + \dot{\mathbf{u}}(t) = Df(\boldsymbol{\xi}(t))\mathbf{u}(t), \quad \mathbf{u}(t) = \mathbf{u}(t + \tau) \quad (9)$$

where $\mathbf{u}(t)$ denotes the corresponding eigenmode of the system. Since the eigenvalue problem is not symmetric the corresponding adjoint eigenmodes may differ:

$$(\lambda + i\omega)\mathbf{v}^*(t) - \dot{\mathbf{v}}^*(t) = \mathbf{v}^*(t)Df(\boldsymbol{\xi}(t)), \quad \mathbf{v}^*(t) = \mathbf{v}^*(t + \tau) \quad . \quad (10)$$

Stabilisation requires to turn the unstable eigenmodes with $\lambda > 0$ into stable modes. Thus a reasonable control method, i.e. a suitable control matrix, should be based on these eigenmodes. We propose an ansatz by an outer product (cf. eq.(4)) which results in

$$\dot{\mathbf{x}}(t) = f(\mathbf{x}(t)) + K\mathbf{u}(t) (\langle \mathbf{v}(t) | \mathbf{x}(t) \rangle - \langle \mathbf{v}(t - \tau) | \mathbf{x}(t - \tau) \rangle) \quad , \quad (11)$$

if the delayed feedback method is employed. The delayed feedback is based on the signal $s(t) = \langle \mathbf{v}(t) | \mathbf{x}(t) \rangle$ where $\langle . | . \rangle$ indicates an inner product. If the state \mathbf{x} contains spatial degrees of freedom the signal includes a spatial integral, i.e. the control force is based on spatial filtering. If the system has large aspect ratio, so that boundary conditions are irrelevant, the spatial components of the eigenmodes are plane waves, and we recover the Fourier filtering technique. But we stress that the unstable eigenmodes $\mathbf{u}(t)$, $\mathbf{v}(t)$ and not the modes which constitute the desired pattern $\boldsymbol{\xi}(t)$ are the relevant quantity. If boundary conditions are important the eigenmodes are no longer plane waves, and the control method (11) takes boundary effects in a proper way into account.

The control performance is again determined by the linear stability of the full system (11) including the control term. Thus we are left with the eigenvalue problem

$$(\Lambda + i\Omega)\mathbf{U}(t) + \dot{\mathbf{U}}(t) = Df(\boldsymbol{\xi}(t))\mathbf{U}(t) + K(1 - \exp[-(\Lambda + i\Omega)\tau])\mathbf{u}(t)\langle \mathbf{v}(t) | \mathbf{U}(t) \rangle \quad . \quad (12)$$

Since the eigenmodes of the free system are mutually orthogonal the solution of eq.(12) is given by the eigenmodes of the free system (8), $\mathbf{U}(t) \equiv \mathbf{u}(t)$, and we

again obtain the eigenvalue equation (7) with $\chi' + i\chi'' = \langle \mathbf{v} | \mathbf{u} \rangle$. Thus coupling and filtering through the eigenmodes of the unstable pattern is as efficient as diagonal coupling where every degree of freedom is measured and controlled.

The analysis just presented explains the efficiency of eigenmode control and yields a generalisation of Fourier filtering techniques for stabilising arbitrary patterns. The control scheme is based on the time dependent eigenmodes. Thus the application of the control force introduces an explicit time dependence as well. Within our analysis we have imposed the condition that the phase of the eigenmode is synchronised with the time dependent pattern that is eventually stabilised. Then the characteristic equation (7) becomes exact and describes the control performance. However, phase lags may occur in autonomous systems, and they adjust themselves during the control process. Moreover, synchronisation phenomena which make the control method even more efficient may become relevant, but the discussion of such features is beyond the scope of the present contribution (cf. [22]).

5 Summary

In contrast to usual control and synchronisation schemes the usage of time-delayed feedback immediately results in high-dimensional dynamical systems even if the free dynamics involves just a few degrees of freedom [23]. For that reason a deeper theoretical understanding of time-delayed feedback schemes on a general level has been developed only recently, although the mathematics is to some extent quite standard [10]. We have sketched the main ideas in section 2, but such approaches are not limited to the original Pyragas scheme. In fact, several modifications have been proposed to circumvent limitations of the original scheme.

Multiple delay times have proven to be fruitful for stabilising highly unstable periodic orbits [24]. An analysis along the lines of section 2 shows that orbits with a large Lyapunov exponent can be stabilised by such approaches. The method is quite robust and easy to implement either by filtering the control signal electronically or by implementing multiple delays using the travelling time of signals, e.g. in optical resonators.

A severe limitation of the conventional delayed feedback scheme results from the fact that only orbits with a complex Floquet exponent can be stabilised [12, 13]. This restriction can be relaxed by means of a time dependent modulation of the control amplitude K [25, 26]. Such approaches have been successfully applied in experiments [25]. The method relies to some extent on the quite complicated structure of the eigenvalue spectrum which explores the infinite dimensionality of the phase space (cf. [27]). As an alternative, recently control loops have been proposed which contain an additional unstable degree of freedom [28]. Although similar ideas are known in control theory, their combination

with time–delayed feedback methods is new and the scheme has not yet been applied in real experiments.

Time–delayed feedback methods do not require the knowledge of the orbit to be stabilised in advance. Just for simplicity we have assumed that its period is a priori known, but that is not a matter of principle. Several empirical and semiempirical schemes have been proposed to find suitable delay times from properties of the control signal [29, 30]. These methods are essentially based on observing dominant peaks in the Fourier spectrum of the control signal and adjusting the delay time within an iteration process. Such schemes can be based on theoretical arguments by a proper analysis of the full delay system including the control force [19]. In particular, quantitative expressions can be derived which relate the periodicity of the control signal with the delay mismatch and the control amplitude.

Time–delayed feedback methods aim at stabilising time periodic states in experimental setups where neither fancy data processing is possible nor some mathematical modelling is available. Such conditions occur frequently in fast experimental systems. It is already known by engineers for decades that control loop latency, i.e. the time lag needed for coupling the control force to the system under consideration, severely limits the efficiency of traditional control methods [31]. Such reservations apply for time–delayed feedback control as well, and one may quantitatively express such a constraint in terms of the control loop latency, the period of the orbit, and its Lyapunov exponent [32].

The analytical approaches for time–delayed feedback methods are restricted to linear stability analysis and thus probe local features of the control scheme. By such an analysis one cannot answer the question which orbit is controlled apart from the trivial observation that the chosen delay time selects a particular class of orbits. In order to answer such questions one has to go beyond linear approaches since one needs to investigate global features like basins of attraction. Such problems, however, are still a considerable mathematical challenge and have not been attacked yet for time–delayed feedback control, although such questions are of utmost importance in experimental contexts.

The investigation of time–delayed feedback schemes for spatially extended systems is still at its beginning. In particular, one has to take explicitly the properties of spatial degrees of freedom into account in order to achieve the full power of time–delayed feedback schemes. On the other hand one should not destroy the simplicity of time–delayed feedback control by invoking an advanced control scheme which is difficult to handle. A proper balance and, in particular, a variety of tests in different experimental situations will prove to be a cornerstone for control of spatio–temporal chaos in the future.

Acknowledgement

The authors are very indebted to Prof. E. Schöll (TU Berlin), A. Amann (TU Berlin) and Prof. J. Holyst (TU Warsaw) for fruitful discussions and to D. Reckwerth (TU Darmstadt) for support in experiments.

References

- [1] L. M. Pecora and T. L. Carroll, *Phys. Rev. Lett.* **64**, 821 (1990).
- [2] E. Ott, C. Grebogi, and Y. A. Yorke, *Phys. Rev. Lett.* **64**, 1196 (1990).
- [3] *Handbook of Chaos Control*, edited by H. G. Schuster (Wiley–VCH, Berlin, 1999).
- [4] K. Ogata, *Modern Control Engineering* (Prentice–Hall, New York, 1997).
- [5] T. Shinbrot, *Adv. Phys.* **44**, 73 (1995).
- [6] H. Kantz and T. Schreiber, *Nonlinear Time Series Analysis* (Cambridge University Press, Cambridge, 1997).
- [7] E. R. Hunt, *Phys. Rev. Lett.* **67**, 1953 (1991).
- [8] A. Azevedo and S. M. Rezende, *Phys. Rev. Lett.* **66**, 1342 (1991).
- [9] K. Pyragas, *Phys. Lett. A* **170**, 421 (1992).
- [10] R. Bellmann, *Differential–Difference Equations* (Acad. Press, New York, 1963).
- [11] M. E. Bleich and J. E. S. Socolar, *Phys. Lett. A* **210**, 87 (1996).
- [12] W. Just, T. Bernard, M. Ostheimer, E. Reibold, and H. Benner, *Phys. Rev. Lett.* **78**, 203 (1997).
- [13] H. Nakajima, *Phys. Lett. A* **232**, 207 (1997).
- [14] W. Just, E. Reibold, and H. Benner, in *Proc. of the 5th Experimental Chaos Conf.*, edited by M. Ding, W. Ditto, A. Osborne, L. Pecora, and M. Spano (World Scientific, Singapore, 2000).
- [15] W. Just, E. Reibold, K. Kacperski, P. Fronczak, J. Holyst, and H. Benner, *Phys. Rev. E* **61**, 5045 (2000).
- [16] W. Just, E. Reibold, H. Benner, K. Kacperski, F. Fronczak, and J. Holyst, *Phys. Lett. A* **254**, 158 (1999).

- [17] *Nonlinear Phenomena and Chaos in Magnetic Materials*, edited by P. E. Wigen (World Scientific, Singapore, 1994).
- [18] J. Becker, F. Rödelsperger, Th. Weyrauch, H. Benner, W. Just, and A. Cenys, Phys. Rev. E **59**, 1622 (1999).
- [19] W. Just, J. Möckel, D. Reckwerth, E. Reibold, and H. Benner, Phys. Rev. Lett. **81**, 562 (1998).
- [20] A. V. Mamaev and M. Saffman, Phys. Rev. Lett. **80**, 3499 (1998).
- [21] E. Benkler, M. Kreuzer, R. Neubecker, and T. Tschudi, Phys. Rev. Lett. **84**, 879 (2000).
- [22] N. Baba, A. Amann, E. Schöll, and W. Just, *Giant improvement of time-delayed feedback control by spatio-temporal filtering* (submitted, 2002).
- [23] J. K. Hale and S. M. Verduyn Lunel, *Introduction to Functional Differential Equations* (Springer, New York, 1993).
- [24] J. E. S. Socolar, D. W. Sukow, and D. J. Gauthier, Phys. Rev. E **50**, 3245 (1994).
- [25] S. Bielawski, D. Derozier, and P. Glorieux, Phys. Rev. A **47**, R2492 (1993).
- [26] H. G. Schuster and M. B. Stemmler, Phys. Rev. E **56**, 6410 (1997).
- [27] W. Just, Physica D **142**, 153 (2000).
- [28] K. Pyragas, Phys. Rev. Lett. **86**, 2265 (2001).
- [29] A. Kittel, J. Parisi, and K. Pyragas, Phys. Lett. A **198**, 433 (1995).
- [30] H. Nakajima, H. Ito, and Y. Ueda, IEICE Trans. Fund. **E80**, 1554 (1997).
- [31] L. Collatz, ZAMM **25/27**, 60 (1947).
- [32] W. Just, D. Reckwerth, E. Reibold, and H. Benner, Phys. Rev. E **59**, 2826 (1999).